Evaluation of Acellular Dermal Matrix Powder–Coated Breast Implants for the Reduction of Capsular Contracture in a Rabbit

Inbong Song , Ilseok Jang , Dayoung Noh , Jungju Kim , Jihyun Lee , Jungkee Kwon *

Posted Date: 15 April 2026

doi: 10.20944/preprints202604.1020.v1

Keywords: capsular contracture; breast implant; acellular dermal matrix

 doi:10.20944/preprints202604.1020.v1

Article

Evaluation of Acellular Dermal Matrix Powder–Coated Breast Implants for the Reduction of Capsular Contracture in a Rabbit

Inbong Song [1,2], Ilseok Jang [2], Dayoung Noh [2], Jungju Kim [2], Jihyun Lee [2] and Jungkee Kwon [1,*]

[1] Department of Laboratory Animal Medicine, College of Veterinary Medicine, Jeonbuk National University, 79 Gobong-ro, Iksan-si, Jeollabuk-do 54596, Republic of Korea

[2] Plastic Material R&D Center, OSSTEM IMPLANT, Magokjungang 12-ro 3, Gangseo-gu, Seoul 07522, Republic of Korea

* Correspondence: jkwon@jbnu.ac.kr; Tel.: +82-63-850-0951

Abstract

Capsular contracture is a common complication following breast implant surgery and is primarily associated with peri-implant fibrotic responses. This study evaluated the effects of an acellular dermal matrix (ADM) powder–coated breast implant on capsular contracture–related outcomes using a rabbit model. Non-textured, smooth-surface breast implants coated with ADM powder were implanted into the subpectoral pocket, and peri-implant tissues were harvested 12 weeks after implantation. Capsule thickness was assessed using hematoxylin and eosin (H&E) staining, while fibrotic changes were evaluated by measuring collagen density in Masson's trichrome (MT)–stained sections. Immunohistochemical analysis was performed to examine the expression of α-smooth muscle actin (α-SMA) and transforming growth factor-β (TGF-β). Compared with conventional breast implants, ADM powder–coated implants demonstrated a reduction in capsule thickness and collagen density, along with decreased expression of α-SMA and TGF-β. These results indicate that ADM powder coating may attenuate peri-implant fibrotic responses and may represent a feasible and cost-effective approach for reducing capsular contracture.

Keywords: capsular contracture; breast implant; acellular dermal matrix

1. Introduction

Capsular contracture is a common complication following breast implant surgery. It is characterized by pathological contraction of the fibrotic capsule formed around the implant and may result in implant deformation, increased firmness on palpation, pain, and aesthetic dissatisfaction [1,2]. Despite advances in implant design and surgical techniques, capsular contracture remains a clinically significant problem [2].

The pathogenesis of capsular contracture is closely associated with persistent inflammatory responses and excessive fibrotic reactions in peri-implant tissues [4,5]. Histological analyses of contracted capsules have demonstrated increased capsule thickness and abnormal extracellular matrix accumulation compared with non-contracted capsules [5,6]. In particular, excessive deposition and altered organization of collagen fibers have been shown to correlate with the severity of capsular contracture [8,9].

Myofibroblast activation is a key cellular event in the development of capsular contracture. Contracted capsules exhibit an increased number of myofibroblasts expressing α-smooth muscle actin (α-SMA), which is associated with cellular contractility and fibrotic remodeling [6,9]. These α-SMA–positive myofibroblasts generate contractile forces and contribute to capsule tightening and

 doi:10.20944/preprints202604.1020.v1

progressive fibrosis [10,11]. Accordingly, α-SMA expression has been widely used as a representative marker for evaluating fibrotic activity in peri-implant capsules [6].

Transforming growth factor-β (TGF-β) plays a central role in regulating fibrotic responses surrounding breast implants. TGF-β signaling promotes fibroblast proliferation, differentiation into myofibroblasts, and collagen synthesis [12,13]. Increased TGF-β expression has been observed in contracted capsules and has been associated with elevated α-SMA expression and enhanced collagen deposition [14,15].

Various strategies have been investigated to reduce capsular contracture, including modifications of surgical techniques and the use of biomaterials to modulate host tissue responses [3,4]. Among these approaches, acellular dermal matrix (ADM) sheets have been widely studied and clinically applied to prevent peri-implant fibrosis. Previous studies have demonstrated that ADM sheets can reduce capsule thickness, modulate collagen organization, and attenuate fibrotic responses around breast implants [17–19]. In addition, meta-analyses have suggested that ADM use in implant-based breast reconstruction is associated with a lower incidence of capsular contracture compared with conventional techniques [17,18].

However, the clinical application of ADM sheets is limited by their high cost and the need for additional surgical procedures, such as complete implant wrapping and fixation [16,18]. These limitations may restrict their widespread use in routine clinical practice.

To address these challenges, alternative strategies utilizing ADM in modified forms have been proposed. ADM powder has emerged as a potential option due to its relative ease of application and potential for cost reduction. Previous studies investigating acellular dermal and extracellular matrix-based scaffolds have demonstrated that acellular dermal components can integrate with host tissues and modulate fibrotic responses even when applied in non-sheet forms, supporting the rationale for this approach [19,20].

Nevertheless, the effects of ADM powder coated directly onto the surface of breast implants on capsular contracture-related parameters, including capsule thickness, collagen deposition, α-SMA expression, and TGF-β expression, have not been sufficiently evaluated.

Therefore, the purpose of this study was to evaluate the efficacy of an ADM powder-coated breast implant in reducing capsular contracture-related outcomes, including capsule thickness, collagen deposition, and the expression of α-SMA and TGF-β, compared with a conventional breast implant, using a rabbit model.

2. Materials and Methods

2.1. Animals

Eight-week-old male New Zealand White rabbits were purchased from Orientbio (Seongnam, Korea) with weight ranging from 2.0-2.5 kg. The rabbits were housed in the animal housing facility of the Medicine and Health Sciences Department of CRONEX Corporation. All rabbits were managed in accordance with institutional ethical guidelines for the care and use of experimental animals at CRONEX (approval number CRONEX-IACUC: 202507003). The rabbit was housed with 12 h cycles of dark and light, were fed a commercial diet and allowed tap water ad libitum and were maintained at a constant environmental temperature (25±2 ℃) and humidity (about 60 %) throughout the study.

After the rabbit entered the facility, the rabbit was acclimated for 2 weeks and then the experiment was conducted. The rabbits were randomly divided into two experimental groups: BI, consisting of rabbits implanted with a non-textured smooth (NTS) surface breast implant, and ADM powder–coated BI, consisting of rabbits implanted with a breast implant with an NTS surface coated with acellular dermal matrix (ADM) powder.

2.2. Implant Preparation

The breast implants (OSSTEM IMPLANT, Seoul, Korea) used in this study had a NTS surface and a volume of 20 cc. All implants were prepared under sterile conditions prior to surgical

 doi:10.20944/preprints202604.1020.v1

implantation. ADM powder was derived from porcine dermis. The porcine dermal tissue was processed using a decellularization procedure to remove cellular components while preserving the extracellular matrix structure. The resulting ADM was subsequently pulverized into a powder form. For preparation of the ADM powder-coated implants, the ADM powder was applied onto the surface of the breast implants by spray deposition to achieve uniform adhesion on the NTS surface (Figure 1). Following the coating process, the implants were subjected to ethylene oxide (EO) gas sterilization prior to use.

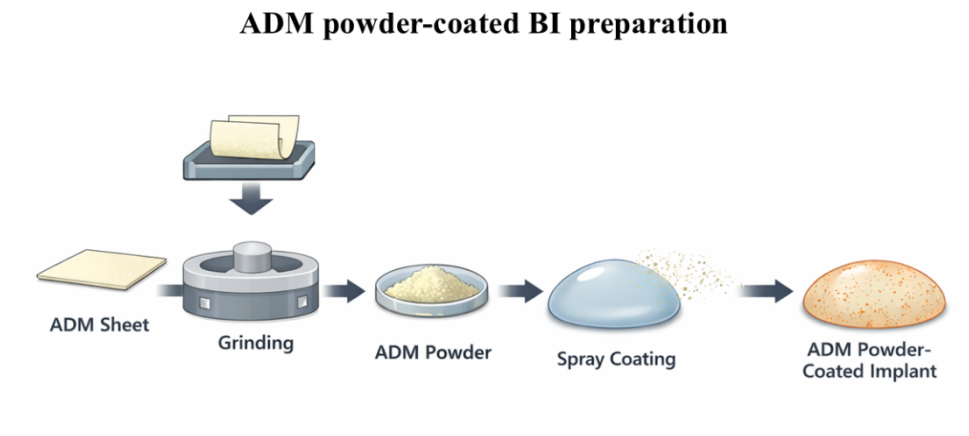

Figure 1. Preparation of ADM powder–coated breast implants. Schematic illustration of the preparation process of acellular dermal matrix (ADM) powder–coated breast implants.

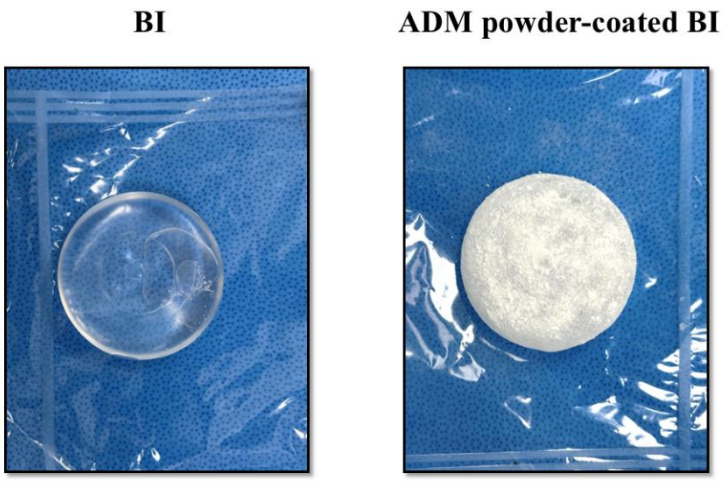

Figure 2. Representative images of breast implants. Representative photographs of the breast implant (BI) and the ADM powder–coated breast implant (ADM powder–coated BI) used in this study are shown.

 doi:10.20944/preprints202604.1020.v1

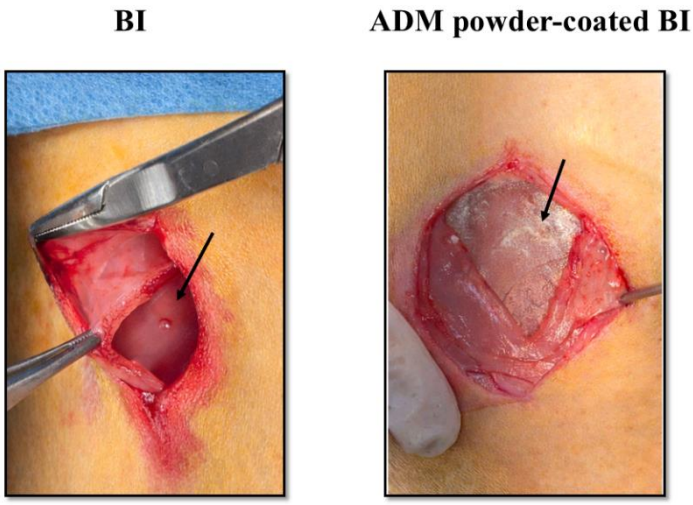

Figure 3. Subpectoral implantation of breast implants in a rabbit model. Representative images showing subpectoral implantation of the BI and ADM powder–coated BI in rabbits. The implants were placed in the subpectoral pocket according to the experimental design.

2.3. Surgical Procedure

All surgical procedures were performed under general anesthesia. After the anesthesia, the dorsal surgical area was shaved, and the skin was aseptically prepared. The animals were positioned to provide adequate exposure to the operative field. A skin incision was created in the dorsal region, and an implant pocket was formed through careful blunt dissection. The implant was placed into a well-defined anatomical plane that is commonly used in rabbit models for peri-implant capsule formation, allowing consistent contact between the implant surface and surrounding soft tissue. The depth and orientation of the pocket were maintained consistently among all animals to minimize procedural variability. Prior to implant insertion, the surgical field was disinfected with a povidone–iodine solution. After placement of the implant according to the assigned experimental group, the incision was closed in layers using absorbable sutures. The surgical site was subsequently disinfected again with povidone–iodine solution. At the predetermined experimental endpoint, the animals were euthanized in accordance with institutional animal care guidelines. Following necropsy, the implanted breast implant and the surrounding peri-implant capsule tissue were carefully harvested to avoid mechanical damage. The collected tissue samples were fixed in neutral buffered formalin for subsequent histological and immunohistochemical analyses.

2.4. Histological Analysis

At 12 weeks following implantation, peri-implant tissues were collected and fixed in 10% neutral buffered formalin for subsequent histological analysis. After fixation, the samples were processed through routine histological procedures and embedded in paraffin. The paraffin-embedded tissues were cut into transverse sections with a thickness of 5 μm relative to the implant surface. Tissue sections were deparaffinized in xylene and subsequently rehydrated through a graded ethanol series. For assessment of general tissue morphology and peri-implant capsule structure, sections were stained with hematoxylin and eosin (H&E). For evaluation of collagen distribution and fibrotic tissue characteristics within the peri-implant capsule, Masson's trichrome staining was carried out using a commercially available staining kit (Abcam, Cambridge, MA, USA). Stained sections were observed using a light microscope (Olympus BX51; Olympus Co., Tokyo, Japan) equipped with a digital imaging system (Olympus DP71; Olympus Co., Tokyo, Japan), and representative images were acquired under identical imaging conditions. Histological assessment was performed by

 doi:10.20944/preprints202604.1020.v1

investigators blinded to the experimental groups. The acquired images were analyzed using Image-Pro Plus software (version 6.0; Media Cybernetics, Rockville, MD, USA) to evaluate collagen distribution within the peri-implant capsule.

2.5. Capsule Thickness

Capsule thickness was assessed using H&E-stained sections. Images of the peri-implant capsule were captured at 100× magnification under a light microscope equipped with a digital imaging system. For each histological image, capsule thickness was measured at six evenly spaced locations along the peri-implant capsule to minimize regional variation. Measurements were performed perpendicular to the capsule surface, and the mean capsule thickness value was calculated for each image. All measurements were conducted using image analysis software (Image-Pro Plus version 6.0; Media Cybernetics, Rockville, MD, USA). The investigators involved in capsule thickness measurement were blinded to the experimental groups during analysis.

2.6. Fibrotic Tissue Formation

Fibrotic tissue formation within the peri-implant capsule was evaluated using Masson's trichrome–stained sections. Images of the peri-implant capsule were obtained under a light microscope equipped with a digital imaging system at a fixed magnification. Fibrosis was quantified by measuring collagen density, as identified by Masson's trichrome staining. Altered collagen architecture has been associated with capsular contracture severity [21]. Collagen density was defined as the proportion of collagen-stained area relative to the total capsule area, reflecting the extent of collagen deposition within the peri-implant capsule. Quantitative analysis was performed using image analysis software (Image-Pro Plus version 6.0; Media Cybernetics, Rockville, MD, USA). All analyses were conducted by investigators who were blinded to the experimental groups.

2.7. Immunohistochemical Analysis

Immunohistochemical staining was performed to evaluate the expression of α-SMA and TGF-β in the peri-implant capsule. Paraffin sections prepared as described above were used for immunohistochemical analysis. Antigen retrieval was performed, and endogenous peroxidase activity was blocked. The sections were incubated with primary antibodies against α-SMA and TGF-β (Abcam, Cambridge, MA, USA) according to the manufacturer's instructions. After incubation with the appropriate secondary antibodies, immunoreactivity was visualized using a chromogenic detection system, followed by counterstaining with hematoxylin. The stained sections were observed at 400× magnification, and representative images were captured using a digital imaging system. The immunopositive areas for α-SMA and TGF-β were analyzed using image analysis software (Image-Pro Plus version 6.0; Media Cybernetics, Rockville, MD, USA). All immunohistochemical analyses were performed by investigators who were blinded to the experimental groups.

2.8. Statistical Analysis

All data are presented as mean ± standard deviation (SD). Statistical analyses were performed using GraphPad Prism software (GraphPad Software, San Diego, CA, USA). Comparisons among experimental groups were conducted using one-way analysis of variance (ANOVA). Differences were considered statistically significant at a p-value of < 0.05 [22].

3. Results

3.1. Effect of ADM Powder–Coated BI on Capsule Thickness in Rabbits

Capsule thickness was evaluated using peri-implant capsule tissues harvested 12 weeks after implantation. Histological assessment was performed on H&E stained sections to examine the morphological characteristics of the peri-implant capsule. Representative histological images from each experimental group are presented in Figure 4. Quantitative analysis revealed a clear difference

 doi:10.20944/preprints202604.1020.v1

in peri-implant capsule thickness between the experimental groups. Compared with the breast implant (BI) group, the ADM powder–coated BI group exhibited a significantly reduced capsule thickness. These findings indicate that ADM powder coating effectively attenuated peri-implant capsule formation in this rabbit model.

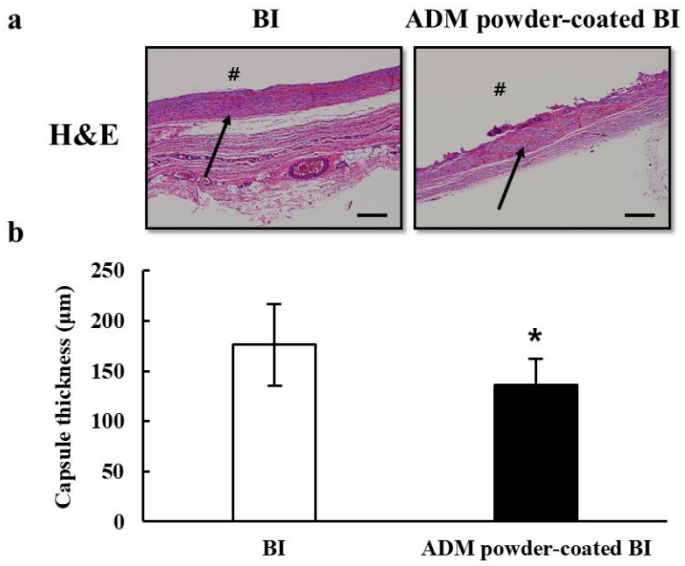

Figure 4. Capsule thickness of peri-implant tissue. Representative hematoxylin and eosin (H&E)–stained sections of the peri-implant capsule and quantitative analysis of capsule thickness 12 weeks after implantation. The mark (#) indicates the implantation site within the peri-implant capsule. Morphological observation of skin. Morphological observation of skin. Photographs of the capsule at 100x magnification. scale bars = 100 μm. Arrows indicate capsule. * $p < 0.05$ compared with BI.

3.2. Fibrotic Tissue Formation in the Peri-Implant Capsule

To assess fibrotic tissue formation within the peri-implant capsule, collagen density was evaluated using Masson's trichrome–stained sections obtained 12 weeks after implantation. Histological examination was performed to visualize collagen deposition and distribution within the peri-implant capsule. Representative images from each experimental group are shown in Figure 5. Quantitative analysis demonstrated a significant difference in collagen density between the experimental groups. Compared with the BI group, the ADM powder–coated BI group showed a significantly reduced collagen density within the peri-implant capsule. These results suggest that ADM powder coating attenuated fibrotic tissue formation and extracellular matrix accumulation around the implant.

 doi:10.20944/preprints202604.1020.v1

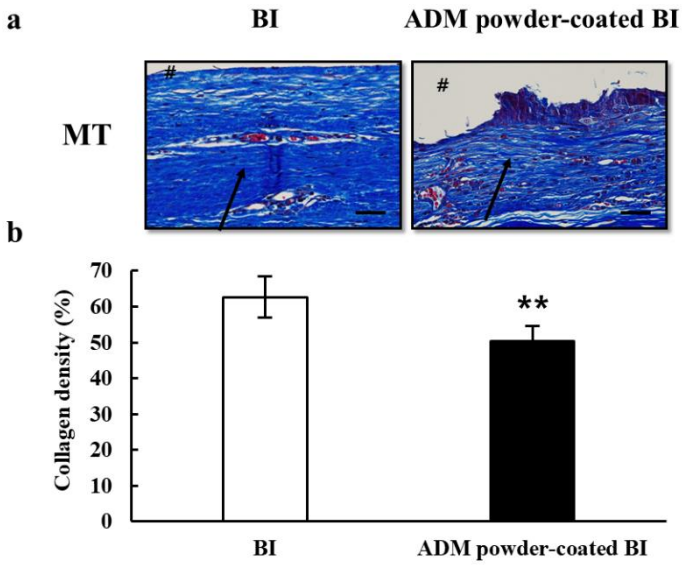

Figure 5. Collagen density in the peri-implant capsule. Representative Masson's trichrome–stained sections of the peri-implant capsule and quantitative analysis of collagen density. Collagen density was significantly lower in the ADM powder–coated BI group compared with the BI group 12 weeks after implantation. The mark(#) indicates the implantation site within the peri-implant capsule. Morphological observation of skin. Photographs of the capsule at 400x magnification. scale bars = 20 μm. Arrows indicate capsule. ** $p < 0.01$ compared with BI.

3.3. α-SMA and TGF-β Immunoreactivity in the Peri-Implant Capsule

Immunohistochemical analysis was performed to evaluate the expression of α-SMA and TGF-β in peri-implant capsule tissues 12 weeks after implantation. Representative immunostained sections and corresponding quantitative analyses are presented in Figures 6 and 7. Compared with the BI group, the ADM powder–coated implant group exhibited significantly reduced α-SMA immunoreactivity within the peri-implant capsule. Quantitative analysis of staining intensity confirmed a statistically significant decrease in α-SMA expression in the ADM powder–coated group, indicating reduced myofibroblast activation and contractile activity in peri-implant tissues. Similarly, TGF-β immunoreactivity exhibited a tendency toward reduction in the ADM powder–coated implant group compared with the BI group, without reaching statistical significance. Overall, the reduced staining intensity and distribution of TGF-β observed in the ADM powder–coated group suggest a potential attenuation of profibrotic signaling within the peri-implant capsule. Taken together, these findings indicate that ADM powder coating is associated with significant suppression of α-SMA expression and a tendency toward reduced TGF-β expression, which is consistent with the observed reductions in capsule thickness and collagen density.

 doi:10.20944/preprints202604.1020.v1

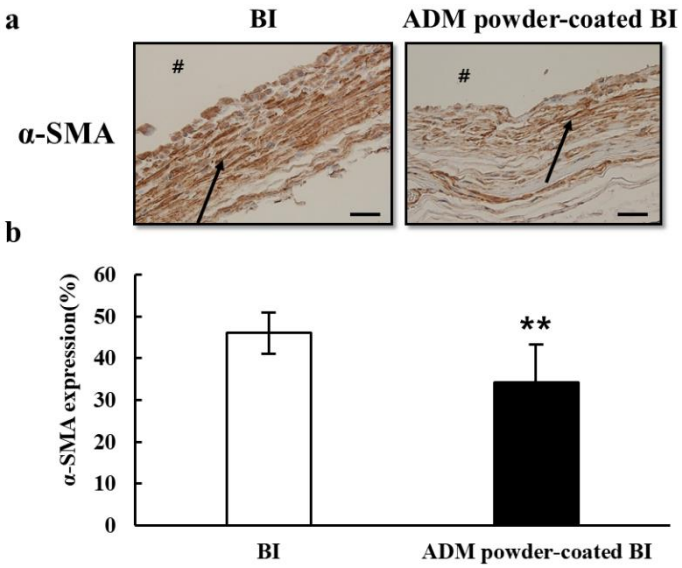

Figure 6. Immunohistochemical analysis of α-SMA expression. Representative immunohistochemical staining images for α-smooth muscle actin (α-SMA) in the peri-implant capsule 12 weeks after implantation. The mark(#) indicates the implantation site within the peri-implant capsule. Morphological observation of skin. Photographs of the capsule at 400x magnification. scale bars = 20 μm. Arrows indicate α-SMA expression. ** $p < 0.01$ compared with BI.

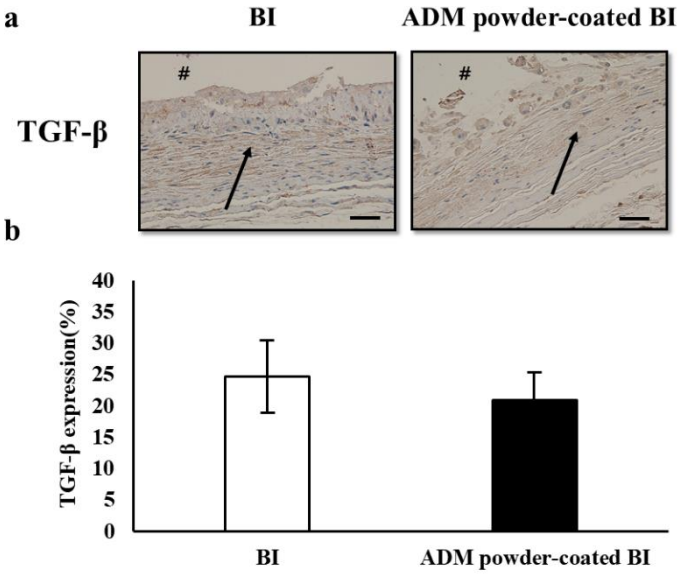

Figure 7. Immunohistochemical analysis of TGF-β expression. Representative immunohistochemical staining images for transforming growth factor-β (TGF-β) in the peri-implant capsule 12 weeks after implantation. The mark(#) indicates the implantation site within the peri-implant capsule. Morphological observation of skin. Photographs of the capsule at 400x magnification. scale bars = 20 μm. Arrows indicate TGF-β expression.

4. Discussion

In the present study, we evaluated the effects of an ADM powder–coated breast implant on capsular contracture–related outcomes using a rabbit model. The main findings were that ADM powder coating was associated with a significant reduction in peri-implant capsule thickness and collagen density, along with visually reduced expression of α-SMA and TGF-β compared with a

 doi:10.20944/preprints202604.1020.v1

conventional breast implant. These results suggest that ADM powder coating may attenuate peri-implant fibrotic responses implicated in capsular contracture [23,24].

Capsular contracture is a fibrotic complication characterized by progressive capsule thickening and excessive extracellular matrix deposition around implants [23–25]. Accordingly, capsule thickness and collagen-rich matrix accumulation are frequently used as histologic outcome measures in preclinical and clinical investigations of contracture severity [25–27]. In the present study, both parameters were significantly reduced in the ADM powder–coated implant group compared with the BI group, supporting the anti-fibrotic potential of ADM delivered via a surface-coating approach.

Collagen accumulation within the peri-implant capsule contributes to increased capsule stiffness and contracture progression [25,26]. Consistent with this concept, collagen density was significantly lower in the ADM powder–coated group, suggesting reduced fibrotic remodeling. Prior work on ADM-assisted implant-based reconstruction has also suggested that ADM can modulate capsule formation and fibrotic tissue responses in peri-implant environments, supporting the biological plausibility of our findings [28–31]. At the same time, clinical evidence indicates that ADM use may be accompanied by procedure-related considerations (e.g., complication profiles), highlighting the importance of developing simplified and standardized delivery formats [32,33].

Myofibroblast activation represents a key cellular event in fibrosis. α-SMA–positive myofibroblasts generate contractile forces and promote matrix remodeling, while TGF-β signaling plays a central role in regulating fibroblast activation and collagen synthesis [34–36]. In the present study, immunohistochemical analysis showed visually reduced staining intensity and distribution of α-SMA and TGF-β in the ADM powder–coated group compared with the BI group. Although these findings were evaluated qualitatively, they are directionally consistent with reduced capsule thickness and collagen density and suggest attenuation of fibrogenic activity.

Several limitations should be considered. First, α-SMA and TGF-β were assessed qualitatively, and future work should incorporate quantitative image analysis and/or molecular assays to better define mechanism. Second, although this study used a rabbit model and a defined endpoint, longer-term and multi-timepoint studies may be needed to evaluate the durability of the anti-fibrotic effects and to correlate histology with macroscopic contracture outcomes.

Importantly, ADM powder coating may alter implant surface characteristics, including surface topography/roughness, which has been reported to influence host tissue responses and the incidence of contracture [37–40]. Implant surface texture can affect early tissue-implant interactions and subsequent capsule development [37–39], and surface-dependent host responses have been demonstrated in vivo [40]. Therefore, future studies will aim to optimize ADM powder particle characteristics and the resulting surface profile to identify coating conditions that most effectively reduce capsular contracture, while separating biological ADM effects from purely topographical effects.

5. Conclusions

Our results suggest that ADM powder–coated breast implants effectively reduce capsular contracture–related responses in a rabbit model. In comparison with conventional breast implants, ADM powder–coated implants demonstrated decreased peri-implant capsule thickness and collagen density, together with visually reduced expression of α-SMA and TGF-β, which are commonly associated with peri-implant fibrotic tissue formation.

These findings indicate that surface coating of breast implants using ADM in a powdered form may serve as a feasible and effective approach to modulate peri-implant fibrotic responses while retaining the biological functionality of conventional ADM sheets. Although additional studies are required to further optimize implant surface characteristics and to elucidate the underlying mechanisms, the present study supports the potential application of ADM powder coating as a practical and cost-effective strategy for reducing capsular contracture in implant-based breast surgery.

 doi:10.20944/preprints202604.1020.v1

Author Contributions: Conceptualization, I.S. and J.K.; methodology, I.S., I.J. and D.N.; validation, D.N. and J.L.; resources, I.J. and JJ.K.; writing—original draft preparation, I.S.; writing—review and editing, I.S. and J.K.; visualization, I.S. and J.L.; supervision, I.J. and J.K.; project administration, JJ.K. All authors have read and agreed to the published version of the manuscript.

Funding: This research received no external funding.

Institutional Review Board Statement: The animal study protocol was approved by the Institutional Ethics Committee of CRONEX (Protocol code: 202507003 and date of approval: 4 July 2025).

Informed Consent Statement: Not applicable.

Data Availability Statement: The data presented in this study are available on request from the corresponding author. The data are not publicly available due to ethical restrictions.

Acknowledgments: This research was supported by OSSTEM IMPLANT Co., Ltd. Fund.

Conflicts of Interest: The authors declare no conflicts of interest.

Abbreviations

The following abbreviations are used in this manuscript:

α-SMA	**α-smooth muscle actin**
TGF-β	**Transforming growth factor-β**
ADM	**Acellular dermal matrix**
NTS	**Non-textured smooth**
H&E	**Hematoxylin and Eosin**
BI	**breast implant**

References

1. Baker, J.L. Augmentation mammaplasty. Plast. Reconstr. Surg. 1978, 61(3), 327–331.
2. Handel, N.; Cordray, T.; Gutierrez, J.; Jensen, J.A. A long-term study of outcomes, complications, and patient satisfaction with breast implants. Plast. Reconstr. Surg. 2006, 117(3), 757–767.
3. Barr, S.; Hill, E.W.; Bayat, A. Functional biocompatibility testing of silicone breast implants and a novel classification system based on surface roughness. J. Mech. Behav. Biomed. Mater. 2017, 75, 548–560.
4. Wilkinson, T.S.; et al. The pathophysiology of capsular contracture: A systematic review. Plast. Reconstr. Surg. 2018, 142(5), 1317–1328.
5. Prantl, L.; Angele, P.; Schreml, S.; et al. Clinical and morphological conditions in capsular contracture formed around silicone breast implants. Plast. Reconstr. Surg. 2007, 120(1), 275–284.
6. Bui, J.M.; Perry, T.; Ren, C.D.; Nofrey, B.; Teitelbaum, S.; Van Epps, D.E. Histological characterization of human breast implant capsules. Aesthetic Plast. Surg. 2015, 39(3), 306–315.
7. Kamel, M.; et al. Fibrosis and inflammation in capsular contracture around breast implants. J. Plast. Reconstr. Aesthet. Surg. 2019, 72(6), 1010–1018.
8. Bisson, M.A.; et al. Collagen organization and density correlate with capsular contracture severity. Plast. Reconstr. Surg. 2013, 131(4), 635–645.
9. Siggelkow, W.; Faridi, A.; Spiritus, K.; Klinge, U.; Rath, W.; Klosterhalfen, B. Histological analysis of capsular contracture: Collagen fiber arrangement and myofibroblast distribution. Plast. Reconstr. Surg. 2003, 112(4), 1188–1196.
10. Tomasek, J.J.; Gabbiani, G.; Hinz, B.; Chaponnier, C.; Brown, R.A. Myofibroblasts and mechano-regulation of connective tissue remodeling. Nat. Rev. Mol. Cell Biol. 2002, 3(5), 349–363.
11. Hinz, B. The myofibroblast: Paradigm for a mechanically active cell. J. Biomech. 2010, 43(1), 146–155.
12. Border, W.A.; Noble, N.A. Transforming growth factor β in tissue fibrosis. N. Engl. J. Med. 1994, 331(19), 1286–1292.
13. Leask, A.; Abraham, D.J. TGF-β signaling and the fibrotic response. FASEB J. 2004, 18(7), 816–827.

 doi:10.20944/preprints202604.1020.v1

14. Prantl, L.; et al. Transforming growth factor-β expression in capsular fibrosis around silicone breast implants. Plast. Reconstr. Surg. 2005, 116(2), 512–520.
15. Baker, S.B.; et al. The role of TGF-β and myofibroblasts in capsular contracture. Plast. Reconstr. Surg. 2003, 112(6), 1713–1721.
16. Zenn, M.R.; Salzberg, C.A. Acellular dermal matrix in breast reconstruction. Plast. Reconstr. Surg. 2012, 130(5 Suppl 2), 70S–79S.
17. Israeli, R.; Feingold, R.S.; Stofman, G.M.; et al. Acellular dermal matrix in breast reconstruction: A meta-analysis. Plast. Reconstr. Surg. 2014, 133(4), 676–689.
18. Sbitany, H.; Sandeen, S.N.; Amalfi, A.N.; Davenport, M.S.; Langstein, H.N. Outcomes analysis of acellular dermal matrix use in breast reconstruction. Plast. Reconstr. Surg. 2015, 135(3), 513–524.
19. Schmitz, M.; et al. Experimental total wrapping of breast implants with acellular dermal matrix reduces capsular fibrosis. J. Plast. Reconstr. Aesthet. Surg. 2013, 66(5), e140–e147.
20. Deeken, C.R.; Eliason, B.J.; Pichert, M.D.; Grant, S.A.; Frisella, M.M.; Matthews, B.D. Histologic evaluation of biologic scaffolds for soft tissue repair. J. Biomed. Mater. Res. B Appl. Biomater. 2012, 100B(2), 483–490.
21. Moyer, K.E.; Ehrlich, H.P. Capsular contracture after breast reconstruction: Collagen fiber orientation and organization. Plast. Reconstr. Surg. 2013, 131(4), 680–685. Bisson, M.A.; McGrouther, D.A.; Mudera, V. Collagen organization and density correlate with capsular contracture severity. Plast. Reconstr. Surg. 2013, 131(4), 635–645.
22. Altman, D.G.; Bland, J.M. Standard deviations and standard errors. BMJ 2005, 331, 903.
23. Spear, S.L.; Baker, J.L. Classification of capsular contracture after prosthetic breast reconstruction. Plast. Reconstr. Surg. 1995, 96, 1119–1123.
24. Headon, H.; Kasem, A.; Mokbel, K. Capsular contracture after breast augmentation: An update for clinical practice. Arch. Plast. Surg. 2015, 42, 532–543.
25. Prantl, L.; Schreml, S.; Fichtner-Feigl, S.; Pöppl, N.; Eisenmann-Klein, M.; Schwarze, H. Clinical and morphological conditions in capsular contracture formed around silicone breast implants. Plast. Reconstr. Surg. 2007, 120, 275–284.
26. Siggelkow, W.; Faridi, A.; Spiritus, K.; Klinge, U.; Rath, W.; Klosterhalfen, B. Histological analysis of silicone breast implant capsules and correlation with capsular contracture. Biomaterials 2003, 24, 1101–1109.
27. Wolfram, D.; Rainer, C.; Niederegger, H.; Piza, H.; Wick, G. Cellular and molecular composition of fibrous capsules formed around silicone breast implants with special focus on local immune reactions. J. Autoimmun. 2004, 23, 81–91.
28. Spear, S.L.; Parikh, P.M.; Reisin, E.; Menon, N.G. Acellular dermis-assisted breast reconstruction. Aesthetic Plast. Surg. 2008, 32, 418–425.
29. Sbitany, H.; Sandeen, S.N.; Amalfi, A.N.; Davenport, M.S.; Langstein, H.N. Acellular dermis–assisted prosthetic breast reconstruction versus complete submuscular coverage: A head-to-head comparison of outcomes. Plast. Reconstr. Surg. 2009, 124, 1735–1740.
30. Kim, I.-K.; Park, S.O.; Chang, H.; Jin, U.S. Inhibition mechanism of acellular dermal matrix on capsule formation in expander–implant breast reconstruction. Ann. Surg. Oncol. 2018, 25, 2279–2287.
31. Lee, K.-T.; Mun, G.-H. Updated Evidence of Acellular Dermal Matrix Use for Implant-Based Breast Reconstruction: A Meta-analysis. Ann. Surg. Oncol. 2016, 23, 600–610.
32. Chun, Y.S.; Verma, K.; Rosen, H.; Lipsitz, S.; Morris, D.; Kenney, P.; Eriksson, E. Implant-based breast reconstruction using acellular dermal matrix and the risk of postoperative complications. Plast. Reconstr. Surg. 2010, 125, 429–436.
33. Tomasek, J.J.; Gabbiani, G.; Hinz, B.; Chaponnier, C.; Brown, R.A. Myofibroblasts and mechano-regulation of connective tissue remodelling. Nat. Rev. Mol. Cell Biol. 2002, 3, 349–363.
34. Hinz, B. The myofibroblast: Paradigm for a mechanically active cell. J. Biomech. 2010, 43, 146–155.
35. Border, W.A.; Noble, N.A. Transforming growth factor beta in tissue fibrosis. N. Engl. J. Med. 1994, 331, 1286–1292.
36. Poeppl, N.; Schreml, S.; Lichtenegger, F.; et al. Does the surface structure of implants have an impact on the formation of a capsular contracture? Aesthetic Plast. Surg. 2007, 31, 133–139.

 doi:10.20944/preprints202604.1020.v1

37. Brohim, R.M.; Foresman, P.A.; Hildebrandt, P.K.; Rodeheaver, G.T. Early tissue reaction to textured breast implant surfaces. Ann. Plast. Surg. 1992, 28, 354–362.
38. Atlan, M.; Nuti, G.; Wang, H.; Decker, S.; Perry, T. Breast implant surface texture impacts host tissue response. J. Mech. Behav. Biomed. Mater. 2018, 88, 377–385.
39. Costerton, J.W.; Stewart, P.S.; Greenberg, E.P. Bacterial biofilms: A common cause of persistent infections. Science 1999, 284, 1318–1322.
40. Tamboto, H.; Vickery, K.; Deva, A.K. Subclinical (biofilm) infection causes capsular contracture in a porcine model following augmentation mammaplasty. Plast. Reconstr. Surg. 2010, 126, 835–842.